Crosstalk in surface electromyogram: literature review and some insights

Original
Crosstalk in surface electromyogram: literature review and some insights / Mesin, L.. - In: AUSTRALASIAN PHYSICAL & ENGINEERING SCIENCES IN MEDICINE. - ISSN 1879-5447. - STAMPA. - 43:2(2020), pp. 481-492. [10.1007/s13246-020-00868-1]

Availability:
This version is available at: 11583/2835234 since: 2020-06-11T17:42:08Z

Publisher:
Springer

Published
DOI:10.1007/s13246-020-00868-1

(Article begins on next page)

Noname manuscript No.
(will be inserted by the editor)

Crosstalk in surface electromyogram

Literature review and some insights

Luca Mesin

Received: date / Accepted: date

Abstract Surface electromyogram (EMG) has a relatively large pick-up volume, reflecting the activity of muscle tissue placed quite far from the electrodes. This could be beneficial when the global muscle activity is of interest, but it is a limitation when selective information is needed. The EMG from muscles that are neighbors of the one of interest is called crosstalk. Its interpretation, identification, quantification and removal have been the objectives of many works in the literature. However, it is still considered as an open problem, with effects that are difficult to predict.

In this paper, the problem of crosstalk is discussed and the main literature is reviewed. Finally, a few recent techniques are introduced that are potentially relevant to quantify or reduce it.

Keywords Surface EMG · Crosstalk · Spatial Filter · Inverse Problem · Source Localization

1 Introduction

Crosstalk in surface electromyogram (EMG) is defined as the signal recorded from electrodes placed on the skin above a muscle of interest (referred to as target muscle), but produced by another. It can pose limitations to different applications of EMG in which selective information from a specific muscle is needed. For example, the detrimental effect of crosstalk was indicated in

L. Mesin
Mathematical Biology & Physiology
Dep. Electronics and Telecommunications
Politecnico di Torino, Turin, Italy
Tel.: +39-011-0904085
Fax: +39-011-0904099
E-mail: luca.mesin@polito.it

the following applications: muscle coordination [1], prosthetic control [2], gait analysis [3], ergonomics for task evaluation [4] and reflexes [5].

Crosstalk was studied in many simulated [6][7][8][9][10] and experimental [11][12][13][14] conditions and different methods were proposed to quantify or to reduce it [15]. The first idea that could be explored to quantify it is that of interpreting the recorded signal as the sum of the EMG from the muscle of interest and crosstalk. Then, the EMG from the muscle producing crosstalk can be recorded (by placing another detection channel over it) and compared to the signal acquired from the muscle of interest (e.g., by cross-correlation). However, this simple idea fails, as surface EMG from the same source changes when recorded from electrodes placed in different locations, due to volume conductor filtering. Furthermore, the filter due to the tissue strongly depends on the anatomy. Moreover, its effect depends on some details of motor unit (MU) action potentials (MUAP), which can be interpreted as the sum of two contributions, one reflecting the propagation of the action potential along the muscle fibres and the latter related to the limited extension of the fibres (and thus to generation and extinction of the action potentials). These problems affected the study of crosstalk and the attempts to interpret it in the literature.

Here, a brief discussion of crosstalk is provided, introducing different notions needed to understand its origin and the rationale behind the processing methods that have been introduced to quantify or reduce it. Specifically, the main results from the literature are mentioned in Section 2. Then, structure-based volume conductor models of surface EMG are discussed, providing some hints for the interpretation of crosstalk (Section 3). Spatial filters are then introduced in Section 4, as a tool for improving selectivity of acquisition. Finally, advanced processing methods are discussed: in the opinion of the author, they are the most promising approaches that have been proposed to quantify or reduce crosstalk (Section 5). Some conclusions and future perspectives are finally given (Section 6).

2 State of the art

The relatively large detection volume of surface EMG questioned the reliability of the information extracted from a target muscle, due to the crosstalk from other muscles. Such a signal may originate from muscles which are located either deeper (ankle flexors and extensors [16], soleus and gastrocnemius [17]), or adjacent (vastus medialis and lateralis [11]) or all around the target muscle (forearm muscles [4][18]).

In applications, crosstalk may be an important concern. For example, the following outcomes were documented in the literature.

1. The appropriateness of using EMG recordings for studying muscle coordination depends on the possibility of decoding neural control strategies of movements, which is hindered by crosstalk [1].

2. In gait analysis, surface EMG indicated activity of rectus femuris even in phases in which intramuscular recordings showed that it was relaxed: this was due to the crosstalk from the vasti [3].
3. The level of crosstalk degraded the extraction of neural control information used to guide myoelectric prostheses with multiple degrees of freedom [2].
4. The study of canine diaphragm EMG was largely affected by crosstalk from the abdominal and intercostal muscles [19].
5. The assessment of human nociceptive withdrawal reflex is usually based on mapping the reflex receptive field by using surface EMG. However, crosstalk can cause erroneous results so that more selective detection systems (called spatial filters, see Section 4) were suggested [20]. The use of such filters was also proposed in many other applications as a way to increase the selectivity of surface EMG (Section 4). However, this improved selectivity may decrease the representativeness of the activity of the target muscle [17].

More examples can be found in a recent review on crosstalk in myograms (EMG and mechanomyogram) [15]. The detrimental and unpredictable effect of crosstalk in applications, promoted technical studies to better observe it and investigate how to quantify or reduce it. The following main indications resulted from these studies.

1. An increase of crosstalk was experimentally observed in the case of a thicker subcutaneous layer [21] (this observation was later justified by simulation models, Section 3).
2. Crosstalk depends strongly on electrode location [22].
3. Based on the assumption that it is produced by muscles at a relative large distance from the recording system (with respect to the target muscle), crosstalk was thought to be highly filtered by the interposed tissue. This suggested that it mainly included low frequency components, which could be removed by a high-pass filter. However, this is not true, as crosstalk is mostly related to non-propagating components reflecting generation and extinction phenomena, which have short duration and include also high frequency contributions [23].
4. Surface EMG is largely affected by the relative position of the detection system and the source (within the active muscles). Thus, crosstalk cannot be quantified by studying the cross-correlation between the EMGs recorded over the two muscles involved [24].
5. Selective spatial filters can reduce the detection volume and hence also the effect of crosstalk [12][25]. However, the optimal configuration of the filter depends on the specific anatomical and physical parameters of the tissues under investigation (studied in many simulation studies, e.g., [6][7][8][9][10]). Thus, the optimal filter could be estimated only by adapting to the specific conditions under study [26].

In summary, most of the literature was limited to observe crosstalk (by measuring it in specific experimental conditions, possibly requiring synchronous acquisition of intramuscular data, or investigating how it changed when the recording system was moved or inter-electrode distance was changed). Simple attempts to quantify (by cross-correlation) or to reduce it (by high-pass filters) were later criticized. The main idea to reduce its effect in applications is to use selective spatial filters, but there is not an optimal configuration, as performances depend on the specific conditions under investigation (e.g., anatomy of the considered subject, conductivity of the tissues, etc.). For a further understanding of these problems and to gain an idea on how to progress in the development of feasible methods for crosstalk management, a deeper understanding of the biophysics behind EMG generation is needed. In the following sections, the generation of surface EMG and the effect of the application of spatial filters are discussed. Then, some advanced methods for crosstalk investigation are introduced.

3 The biophysical interpretation of the generation of surface EMG

Modelling surface EMG is useful to test ideas on simulated experiments and to check accuracy of signal processing algorithms. It supports the estimation of not accessible parameters (inverse problem, [27]), the optimization of spatial filters [9][28][29], the design of algorithms [30][31] and the interpretation of experiments [7][32][33][34].

Some EMG models are phenomenological, which means that they simulate a signal with similar properties, but without describing the underlying deterministic laws of the system generating it. For example, autoregressive linear models adapt the parameters of a non-stationary stochastic process to the data to be represented [35].

Here, we are interested in structure-based models, which describe the biophysical mechanisms of the simulated system. The contraction of fibres of a striated muscle is primed by the intra-cellular action potential (IAP), which is generated at the endplate of a muscle fibre, propagates along it in opposite directions toward the two fibre ends (usually, the tendons), where it extinguishes. The IAP is a bioelectric source constituted by ionic fluxes across the fibre membrane (sarcolemma) that, due to nonlinear diffusion (described by cable theory), induces the excitation of subsequent portions of the membrane over time, thus travelling along the sarcolemma [36]. The IAP induces a potential in the surrounding physiological tissues, as it is a current source embedded into electrically conductive tissues. The diffusion of the electric potential in the tissues leads to a volume conduction problem. As frequencies involved in the problem are small (so that they don't reach the range in which tissue permittivity is relevant [38]), a quasi-static approximation is usually considered. Thus, the equation of electrostatics (Poisson equation) is studied to simulate the potential induced by the IAP into the tissues, under conditions of insulation at the skin surface (conductivity of air is neglected). The potential computed over the skin is finally used to simulate surface EMG corresponding to an IAP. In this way, considering the generation, propagation and extinction of the IAP, a single fibre action potential (SFAP) can be obtained. Adding

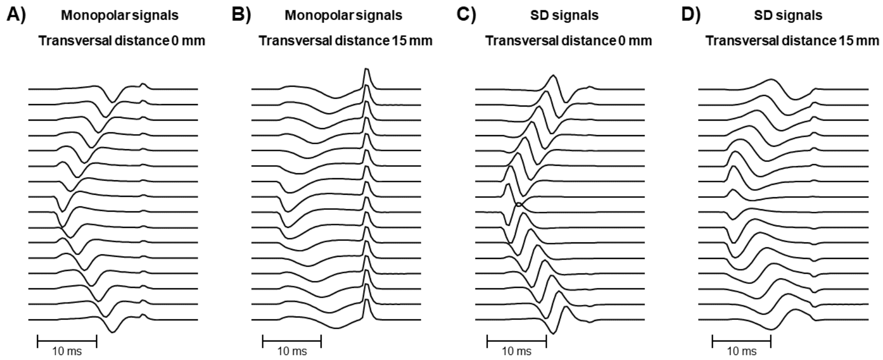

Fig. 1 Example simulations of single fibre action potentials for fibres aligned to the detection array and placed at two different transversal distances from it (plane layer model; skin thickness 1 mm and conductivity 0.022 S/m, fat thickness 3 mm and conductivity 0.04 S/m, muscle extending to minus infinity with transverse and longitudinal conductivities of 0.09 and 0.4 S/m, symmetrical fibre with 60 mm of semi-length, 3 mm deep within the muscle, rectangular electrodes of 3 mm x 1 mm, inter-electrode distance of 5 mm, 16 channels of different spatial filters). A) Monopolar potential, for a fibre placed under the electrodes. B) Monopolar potential of a fibre at a transversal distance of 15 mm from the detection array. C) Single Differential (SD) potential, for a fibre placed under the electrodes. B) SD potential of a fibre at a transversal distance of 15 mm from the detection array.

more SFAPs, a MUAP can be simulated. Then, by describing the spatial and temporal recruitment strategy of MUs, an interference EMG can be simulated [39].

For a better understanding of crosstalk, we are especially interested in the description of the IAP (mainly, its generation and extinction) and volume conductor. Indeed, the effects on single MUAPs are simply summed-up when more MUs are considered in an interference EMG.

The volume conductor is not homogeneous (it includes layers of different tissues, with different electrical properties, like skin, fat, bone and muscle, possibly including inhomogeneity due to complex geometry or variation of parameters) and anisotropic (in particular, muscle fibres are more conductive along than across their direction). Both analytical [40][41] and numerical methods [7][42][43] have been proposed to simulate different volume conductors. The general indication is that the recorded signal is largely affected by the geometry and conductivity of the volume conductor, which could include inhomogeneities, different thickness of tissues and directions of the fibres (which could be curved or go deep). An extensive review of volume conductor simulation is provided in [44] and many applications of models in the interpretation of EMG are discussed in [45].

The simplest volume conductor that can be considered is a homogeneous and isotropic tissue. It is very far from real physiological tissues, but it allows to get preliminary indications on how the potential decays in space. The impulse response (or Green function) of Poisson equation for a homogeneous and isotropic volume conductor is inversely related to the distance from the detection point to the source. A propagating IAP can be approximated by a tripole that, at some distance from it (much larger than the extension of the tripole, which is in the order of 5 mm), i.e., in far field conditions, shows a potential which is about the second derivative of the impulse response. This means that it decays proportionally to the cubic of the distance. On the other hand, generation and extinction of the IAP can be approximated as dipole sources [44]. The far field effect of a dipole is the first derivative of the impulse response, so that it decays in space with the square of the distance. Thus, when increasing the distance from an active muscle fibre, the corresponding potential waveform that could be recorded is distorted, with the propagating contribution decaying rapidly and the non-propagating one (related to generation/extinction) reducing slowly. This reflects into different shapes of MUAPs recorded from different locations and thus to the difficulty in quantifying crosstalk by cross-correlation of EMGs recorded over the muscle producing it and the one of interest. Moreover, the non-propagating components increase their relative importance when the EMG is recorded more and more distant from the active muscle. For this reason, crosstalk EMG is largely constituted by non-propagating components. Examples of simulated monopolar and single differential (SD) SFAPs obtained considering a fibre either under the detection system or transverse displaced is shown in Figure 1. The relative contribution of non-propagating components is largely increased when the fibre is displaced.

4 Spatial filters

More electrodes placed close to each other are used to detect high-density surface EMG. The potentials under these electrodes can be linearly combined, obtaining what is called a spatial filter. The name is appropriate when recording a potential travelling under the electrodes, as this propagation allows the filter to apply a convolution operation on the action potential. However, for the action potential waveform to propagate without distortion, the volume conductor should be space invariant [42] and the length of the muscle fibres should be infinite. As these conditions cannot be perfectly matched, predicting the effect of the application of a spatial filter is not trivial. In particular, the effect on generation and end of fibre components (or other perturbations to the propagating waveform) should be tested carefully.

Different filters have been proposed [46]: the single differential (SD) computes the difference between the potentials of two electrodes, approximating a spatial derivative; the double differential (DD) approximates the second derivative (with a negative sign); the Laplacian or normal double differentiating filter (NDD) approximates (up to the sign) the Laplacian operator.

Different spatial filters can be compared in terms of their selectivity [47]. It can be intended as the ability of recording the potentials from sources located in a specific region. We call detection volume the region from which a reliable potential can be recorded (i.e., with amplitude much larger than the noise, so that the activation of a specific source can be identified). A selective filter is focused on a small detection volume. Usually, by increasing the number of electrodes (whose recorded potentials are linearly combined) and reducing the inter-electrode distance, the detection volume of the filter is reduced. However, as mentioned above, this is not true in general, as performances depend on the specific case under study. Selectivity can be measured in terms of the ability of removing contributions from deep sources or from regions that are transversely displaced with respect to the center of the detection channel. A longitudinal selectivity can also be defined, in terms of the ability of recording a short spike corresponding to a single source, so that it can be better separated from other asynchronous contributions in the signal [46].

Spatial filters may have different selectivity to propagating and non-propagating terms [48]. For example, in Figure 1, notice the ability of SD filter to reduce the non-propagating components, which are much more evident in the monopolar recordings. However, this selectivity depends on the specific anatomy [9][47]: thus, as mentioned above, a recording system which is optimal in all cases cannot be designed. A filter to be optimal should be adapted to the case under investigation [26].

Selectivity is beneficial to focus on a specific muscle region under the detection channel, thus reducing crosstalk. However, the small selected muscle region could provide poor information on the activity of the whole muscle, as other portions could behave differently [49]. Thus, improved selectivity may decrease the representativeness of the activity of the target muscle [17]. This could be due either to the use of selective detection systems or even to a localized amplitude distribution of MUAPs, as in the case of some pinnate muscles like gastrocnemius [50][51]. The problem of representativeness was also noted for the intramuscular recordings, which are indeed very selective: multiple recordings were suggested to better represent the activity of some muscles [52].

5 Signal processing

As basic methods to face crosstalk, trying to reduce it (by high-pass filtering) or to quantify it (by cross-correlation or coherence), were not so effective, alternatives were proposed, based on advanced signal processing techniques. In the following, three main ideas are discussed: blind source separation, adaptive spatio-temporal filtering and inverse modelling.

5.1 Blind Separation of EMG from target and crosstalk muscles

Blind Source Separation (BSS) is a statistical theory aiming to separate different sources from available data in which their contributions are mixed (mixtures or observations) [53][54]. Different models for the data have been studied, e.g., the linear instantaneous [13] and the convolutive [55]. In the problem to be solved, both the sources and their weights (or impulse responses, in the convolutive model) are unknown for each mixture. However, successful separation can be achieved by imposing some statistical property of the sources to be found, if the number of mixtures is at least equal or (better) larger than that of the sources. Popular requirements imposed to the sources are to be either uncorrelated (considered in principal component analysis, PCA) or independent (independent component analysis, ICA).

An example of BSS technique to separate crosstalk from the EMG of the target muscle was proposed in [13]. The method assumes that the recorded data are linear instantaneous mixtures of the signals produced by the investigated muscles, which are the sources to be separated. Thus, the model is the following

$$\mathbf{x}[t] = \mathbf{A}\mathbf{s}[t] + \mathbf{n}[t] \tag{1}$$

where $\mathbf{x}[t] = [x_1[t], \cdots, x_m[t]]^T$ is the vector of m mixtures, $\mathbf{s}[t] = [s_1[t], \cdots, s_n[t]]^T$ is the vector of n sources, $\mathbf{A}$ is the full rank mixing matrix of size $m \times n$ with $m \geq n$ and $\mathbf{n}[t]$ is the additive white Gaussian noise vector, assumed to have same power σ^2 in all mixtures. Notice that the order of the sources and their amplitudes cannot be determined, as the two unknowns are multiplied (ambiguities of the BSS problem).

In principle, the sources could be computed by (pseudo-)inverting the mixing matrix, once it is estimated. The mixing matrix is factorized as $\mathbf{WA} = \mathbf{U}$, where $\mathbf{W}$ is orthogonal and $\mathbf{U}$ is unitary. The method is called second order blind identification (SOBI) and extends PCA by applying a whitening transformation $\mathbf{W}$ and then by recovering the rotation matrix $\mathbf{U}$ [56]. It can be split into the following two steps.

– *Whitening*. The whitening matrix $\mathbf{W}$ is constructed such that

$$\mathbf{W}\mathbf{A}\mathbf{A}^T\mathbf{W}^T = \mathbf{I} \tag{2}$$

The matrix $\mathbf{A}\mathbf{A}^T$ can be determined from the covariance matrix of observations

$$\hat{\mathbf{R}}_{xx} = \frac{1}{T}\sum_{t=1}^{T} \mathbf{x}[t]\mathbf{x}[t]^T \tag{3}$$

which can be written as

$$\hat{\mathbf{R}}_{xx} \approx \mathbf{A}\hat{\mathbf{R}}_{ss}\mathbf{A}^T + \sigma^2\mathbf{I} \tag{4}$$

where $\hat{\mathbf{R}}_{ss}$ is the covariance of the sources. In [13], it was assumed to be the identity matrix (thus, PCA is considered, so that sources are assumed to be orthogonal; moreover, their arbitrary energy was fixed to 1). Thus, the matrix $\mathbf{A}\mathbf{A}^T$ in equation (2) can be written as

$$\mathbf{A}\mathbf{A}^T \approx \hat{\mathbf{R}}_{xx} - \sigma^2\mathbf{I} \tag{5}$$

An estimate $\hat{\sigma}^2$ of the noise variance is the average of the $m - n$ smallest eigenvalues of $\hat{\mathbf{R}}_{xx}$. The spatial whitening matrix $\mathbf{W}$ can now be written in terms of the n largest eigenvalues $\lambda_1, \cdots, \lambda_n$, corresponding to the eigenvectors $\mathbf{h}_1, \cdots, \mathbf{h}_n$ of $\hat{\mathbf{R}}_{xx}$

$$\mathbf{W} = \left[\frac{1}{\sqrt{\lambda_1 - \hat{\sigma}^2}} \mathbf{h}_1, \cdots, \frac{1}{\sqrt{\lambda_n - \hat{\sigma}^2}} \mathbf{h}_n \right]^T \tag{6}$$

– *Rotation.* The application of the whitening matrix $\mathbf{W}$ to the observations provides the whitened observations

$$\mathbf{z}(t) = \mathbf{W}\mathbf{x}(t) = \mathbf{U}\mathbf{s}(t) + \mathbf{W}\mathbf{n}(t) \tag{7}$$

The rotation matrix $\mathbf{U}$ is obtained by diagonalizing the covariance matrix of the whitened observations (thus, imposing that the sources are uncorrelated for each time lag)

$$\hat{\mathbf{R}}_{zz} \approx \mathbf{U}\hat{\mathbf{R}}_{ss}(\tau)\mathbf{U}^T, \qquad \tau \neq 0 \tag{8}$$

Notice that the time lag was assumed to be different from zero to remove the noise contribution. The matrix $\mathbf{U}$ could be obtained from a single arbitrary choice of the time lag. More stable alternatives were introduced, e.g., sampling more time lags and choosing the matrix that allows to get their joint diagonalization which is the best under some optimality condition (like the reduction of a norm of the off diagonal elements [54]; an optimization problem in the time-frequency domain was considered in [13]). Once obtained the whitening and rotation matrices, the mixing matrix is obtained as

$$\mathbf{A} = \mathbf{W}^{\#}\mathbf{U} \tag{9}$$

(where $\mathbf{W}^{\#}$ is the Moore-Penrose pseudoinverse of $\mathbf{W}$) and the sources can be estimated.

This algorithm was applied in [13] to separate the contributions of two forearm muscles, which allow rotation and flexion of the wrist (i.e., pronator teres and flexor carpi radialis). As these muscles are close, the separation of their EMG is very difficult. Signals were detected over the two muscles and in between. The algorithm was able to largely reduce crosstalk, allowing to better identify the periods in which different muscles were either active or silent.

In the example shown in Figure 2, two distinct muscles were simulated with force level of 20% MVC. Three mixtures were available, taken from monopolar channels placed over each of the two muscles and in between. SOBI method was applied to the 3 mixtures to separate the contributions of the two muscles. Notice the partially overlapped spectra, that would make very complicated the separation with simple filtering techniques.

The considered BSS method has some limitations. It is based on the assumption that recorded data are linear, instantaneous mixtures of uncorrelated sources. The assumption of linearity and instantaneity is not strictly valid: MUAPs have shapes that strongly depend on the detection points of the channels recording the different mixtures (as discussed in Section 3). Moreover, sources could be correlated in some applications, as in the case of functional coordination or synergy reflecting the presence of common descending drive

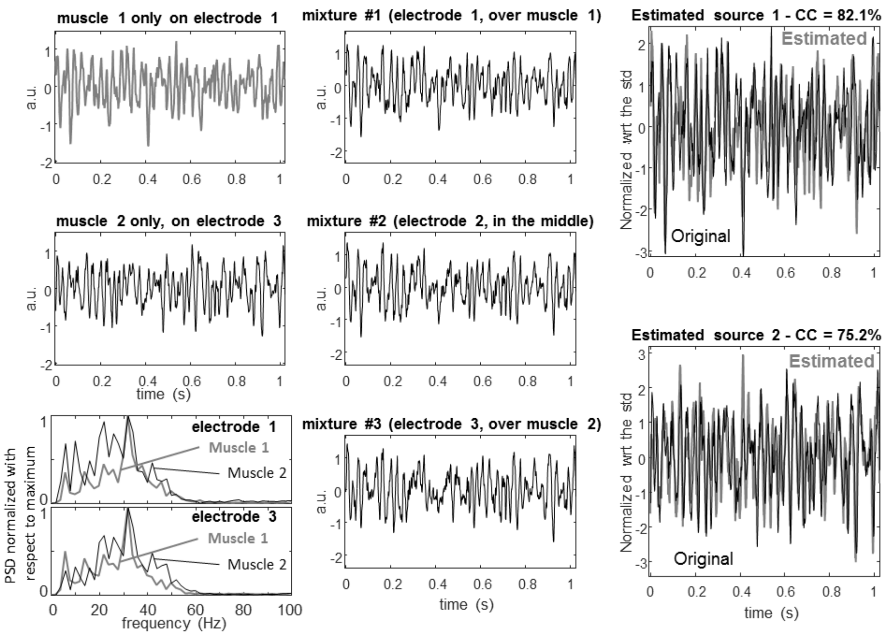

Fig. 2 Second order blind identification (SOBI) method applied to reduce crosstalk between two muscles (both with contraction levels of 20% MVC). Simulations of monopolar signals detected over the two muscles and in between were considered (same simulator as in Figure 3, considering the 3 central channels). Signals from single muscles (from 2 electrodes) and the PSDs (of EMGs from both single muscles recorded from 2 electrodes) are shown on the left, the three mixtures in the middle and the result of the reconstruction superimposed to the single muscles signals on the right (1 s is shown out of the 5 simulated EMGs). The same figure is shown in [37].

shared by MU pools of the different muscles. Moreover, the algorithm cannot be easily integrated in real time applications involving non-stationary data, as the mixing matrix changes in time and should be updated processing the data that are acquired. Thus, the method is quite difficult to employ in applications and it haven't found great outcome till now.

5.2 Optimal spatio-temporal filter

The main approach to reduce crosstalk in applications consists in using selective spatial filters, as they are simple to use and process data in real time. Due to their small detection volume, these filters largely reduce the signal from other muscles. However, also most of the EMG produced by the target muscle is discarded. As mentioned above, this poses a problem of representativeness [17]. Moreover, selective filters could be not available for some applications in which a few, large electrodes are commonly used. An innovative approach was followed in [26], where three principles were considered.

1. The EMG of the muscle of interest had to be retained and the one coming from nearby muscles had to be reduced as much as possible.
2. The method had to be simple and stable in order to be feasible for applications (i.e., real time and useful also for simple experimental protocols using a few not selective detection channels).
3. The method had to be adapted to the considered condition (depending on anatomy, conductivity of the volume conductor, electrode type and location, etc.).

A filter was considered, in order to get a real time processing. The filter was optimized on a training set of signals, including selective activations of the different muscles involved (target and crosstalk muscles). An optimization problem was implemented, reducing crosstalk, but still maintaining the signal from the target muscle. An energetic measure was considered to define the cost function for the optimization problem, which allowed to get a solution in analytical form.

Specifically, indicate with $S_i(t)$ and $C_i(t)$ (with the subscripts indicating the i^{th} channel) the signals recorded either during a selective contraction of the target or of the crosstalk muscles, respectively. Notice that the channels should be placed over both the target muscle and the one(s) producing crosstalk, in order to record useful information for the filter to work properly. The signal to crosstalk ratio (SCR) was defined as

$$SCR = 10\log_{10}\frac{\left\|\sum\limits_{i=1}^{NT} w_i S_i(t)\right\|}{\left\|\sum\limits_{i=k}^{NT} w_k C_k(t)\right\|} \tag{10}$$

where $\{w_i\}$ is the set of weights of the filter, whose sum is imposed to be zero, unless the considered channels already removed common mode interference. Now, an optimal spatial filter (OSF) can be obtained choosing the weights in order to maximize the SCR on the training set. Maximizing the argument of the logarithmic function is sufficient (as the logarithm is monotonic), so that the problem can be converted into the maximization of the following functional

$$J(\mathbf{w}) = \frac{\left\|\sum\limits_{i=1}^{NT} w_i S_i(t)\right\|}{\left\|\sum\limits_{i=k}^{NT} w_k C_k(t)\right\|} = \frac{\mathbf{w}\mathbf{S}^T\mathbf{S}\mathbf{w}}{\mathbf{w}\mathbf{C}^T\mathbf{C}\mathbf{w}} = \frac{\mathbf{w}R_S\mathbf{w}}{\mathbf{w}R_C\mathbf{w}} \tag{11}$$

where R_S and R_C are the autocorrelation matrices of signal and crosstalk, respectively. As this functional is invariant under scaling of the vector of weights, its maximization is equivalent to the following constrained optimization problem

$$\begin{cases} \underset{\mathbf{w}}{\text{argmax}}\frac{1}{2}\mathbf{w}R_S\mathbf{w} \\ \text{subject to } \ \mathbf{w}R_C\mathbf{w} = 1 \end{cases} \tag{12}$$

which can be solved studying the following Lagrangian

$$L_p = \frac{1}{2}\mathbf{w}R_S\mathbf{w} + \frac{1}{2}\lambda(1 - \mathbf{w}R_C\mathbf{w}) \tag{13}$$

Karush-Kuhn-Tucker (KKT) conditions lead to the eigenvalue problem

$$R_S\mathbf{w} = \lambda R_C\mathbf{w} \qquad \Rightarrow \qquad R_C^{-1}R_S\mathbf{w} = \lambda\mathbf{w} \tag{14}$$

The change of variables $\mathbf{v} = R_S^{1/2}\mathbf{w}$ allows to obtain a problem involving a symmetric and positive matrix with orthogonal eigenvectors and positive eigenvalues

$$R_S^{1/2}R_C^{-1}R_S^{1/2}\mathbf{v} = \lambda\mathbf{v} \tag{15}$$

The eigenvectors indicate directions of projections along which the functional becomes

$$\begin{aligned} J(\mathbf{w}_k) &= \tfrac{\mathbf{w}_k R_S \mathbf{w}_k}{\mathbf{w}_k R_C \mathbf{w}_k} = J(R_S^{-1/2}\mathbf{v}_k) = \\ &= \tfrac{\mathbf{v}_k R_S^{-1/2} R_S R_S^{-1/2}\mathbf{v}_k}{\mathbf{v}_k R_S^{-1/2} R_C R_S^{-1/2}\mathbf{v}_k} = \tfrac{1}{1/\lambda_k} = \lambda_k \end{aligned} \tag{16}$$

where $\mathbf{w} = R_S^{-1/2}\mathbf{v}$ and λ_k - $\mathbf{v}_k$ is the k^{th} eigenvalue - eigenvector pair of (15). From (16), the weights corresponding to a maximal SCR are the elements of the eigenvector associated to the largest eigenvalue.

The OSF was generalized including also past values of the EMG data, so that, for each channel, a FIR filter was used instead of a simple amplitude scaling [26]. The filter obtained maximizing the SCR including present and past data was called Optimal Spatio-Temporal Filter (OSTF), as it operates both in time and in space [26]. The delay between subsequent samples and the order of the temporal filters are two parameters that can be tuned, e.g., by improving the performances on a validation set.

The possibility of choosing the weights allows to adapt the filter to the specific anatomy under study. In the specific simulations shown in [26], the FIR filters processing data acquired over the target and crosstalk muscles were stop-band, reducing high frequency noise and keeping the signal of interest. In particular, the filter processing the signal over the muscle producing crosstalk selected the frequency band of its contribution recorded over the target muscle. Thus, the filter appeared to have the effect of estimating the contribution of crosstalk to be subtracted from the EMG recorded over the target muscle.

If the training data are representative of the test signals (e.g., they were recorded during contractions with similar range of motion, force, velocity, etc.), the filter should be optimal also for them. In [26], the filter showed to be robust also to perturbations of the training set. The following conditions were tested: 1. reduced force level so that only some MUs were recruited during training, 2. not selective contractions so that the muscle assumed to be at rest produced a low level activity, 3. reduction of conduction velocity (CV) as a myoelectric manifestation of fatigue. Thus, during the optimization procedure, the filter seemed to adapt to the anatomy and geometry of the volume conductor, without being much affected by the specific training EMG, which depended on the specific temporal and spatial recruitment of MUs and on their fatigue level (reflected in their CV).

Two examples of application were shown in [26]. The method showed to be able to reduce the bias on CV estimation induced by crosstalk. Moreover, it was able to improve the estimation of the simulated force level of the target muscle in the presence of crosstalk. Preliminary tests on experimental data were also shown.

This method is real time and stable. It has the limitation of requiring a preliminary phase of training, during which selective contractions of the involved muscles should be investigated. However, it works even considering a few detection channels, having the potentiality of finding applications also in conditions in which simple recording systems are used (i.e., in many applicative studies in ergonomics, sport science, clinics, gait analysis, or myoelectric prosthesis, in which usually the sophisticated research recording systems are not used).

An example of application of the OSTF is shown in Figure 3. The filter was trained on simulated selective contractions of either of two muscles, considering epochs of stationary EMG at different force levels. Then, it was applied on simulated contractions with variable force levels. The contribution of the crosstalk muscle was reduced: the envelope of the surrogate channel clearly indicates the three bursts of activity, whereas a raw SD channel reflected the contributions of both muscles.

5.3 Estimation of crosstalk by inverse modelling

In principle, crosstalk could be removed if the different contributions of the recorded EMG could be associated to specific sources within the muscles. In such a case, the contributions reflecting the activity of MUs not located in the target muscle could be removed.

The position of the active regions could be extracted from high-density surface EMG by estimating the location of the current sources generating the surface potential. This is an inverse problem, which could be considered as the reverse of the problem of simulating the signal given the sources (Section 3). This latter problem is considered as the direct one, as it simulates the effect once the cause is known. In inverse problems, given the effect (i.e., the recorded data), the cause generating it (i.e., the activity of current sources within the muscle) is sought. This problem was extensively studied in the field of surface electroencephalogram (EEG) [57]. In the field of EMG, some studies have been proposed [58][59][60][61][62][63][64][65]. Most of these methods are computationally intensive. For example, the position of the MU generating a specific MUAP (extracted by a decomposition algorithm) was estimated in [62] considering that the amplitude decay of the potential in a direction transverse to the fibres is slower for deeper MUs. To apply this method to an interference signal, the contributions of different MUs should be first identified, which requires the application of algorithms with high computational cost. Other

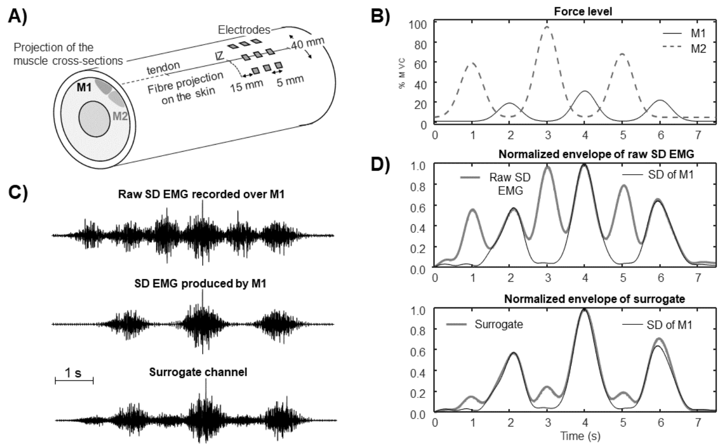

Fig. 3 Application of the optimal spatio-temporal filter (OSTF) to reduce crosstalk (only two samples in time were included in the FIR filter). A) Volume conductor used for the simulations. Interference EMGs from two muscles (M1 and M2) were simulated as in [26]. Monopolar signals were acquired from 9 electrodes, placed over either of the two muscles and in between. B) Force levels of the two muscles. C) Assuming the signal from M1 is of interest, the raw signal from the single differential (SD) channel placed over M1 and closer to the innervation zone is shown, together with the corresponding SD EMG produced by M1 only and the surrogate data obtained by the OSTF (trained using selective, stationary EMGs of 5 s at 20, 40, 60, 80% MVC, for each muscle). D) Envelope (absolute value low-pass filtered at 2 Hz) of the SD raw data and of the surrogate over time, compared to that of the SD signal from M1.

approaches are based on intensive simulations by the finite elements method (FEM), which were fit to experimental data to locate the sources producing interference EMG [58][59][60][63][64][65].

As a low cost alternative, a method was proposed to search for a fit of the data using a set of available waveforms, each representing the activity of a specific portion of the muscle [61]. It is interesting, as it is feasible for real time applications, like prosthesis control, rehabilitation guidance with a biofeedback or crosstalk removal for improving the estimation of EMG indexes (amplitude, spectral properties, CV), force level, muscle synergies or load sharing. The method is based on the following modelling assumption

$$b\,(x,t) = \sum_{n=1}^{N_R} \sum_{k=1}^{N_\tau} X_{n,k} a_n\,(x, t - \tau_{nk}) \tag{17}$$

where $b\,(x,t)$ is the recorded EMG, x is the space variable (indicating the position of the recording channels), t is the time variable, τ_{nk} is a delay (N_τ is the number of considered delays) and $a_n(x,t)$ are N_R basis waveforms, each representing the EMG response to the activity of a source with a specific location. They can be obtained by either simulations or experimental measurements (e.g., by spike triggered averaging technique, i.e., averaging epochs of surface EMG centred on the spikes identified by decomposing the intramuscular EMG jointly acquired). The unknowns are the coefficients $\{X_{n,k}\}$. If the coefficient $X_{n,k}$ is positive, it indicates that there is an activity from the n^{th} region at a delay τ_{nk}.

Equation (17) can be rewritten in matrix form

$$AX = b, \tag{18}$$

where the columns of A contain the basis waveforms, b is the vector of the measurements and X collects the unknowns. This problem cannot be solved, as A is not square (as more recordings than unknowns are usually considered to get more robust estimations). Moreover, the measurement vector b cannot be represented as the sum of the basis waveforms, as it includes noise and only few basis waveforms are considered. Thus, the problem was solved in the least mean squared sense after introducing Tikonov regularization to improve stability to noise

$$\min_X \|AX - b\|^2 + \alpha\|X\|^2 \tag{19}$$

where the first term is the residual norm (measuring the error in data fitting) and the second is the solution norm, imposing the energy of the solution to be small (hindering the selection of an oscillating solution, reflecting large phase cancellations; on the other hand, the essential solution including only few sources is selected, accepting a larger residual variance in fitting the data, with such a residual error ideally reflecting the contribution of noise). The solution was imposed not to show large oscillations by properly choosing the penalization parameter α which was set to be one thousandth of the maximum eigenvalue of the matrix $A^T A$. The problem has the following analytical solution

$$X = (A^T A + \alpha I)^{-1} A^T b \tag{20}$$

This solution can have unphysical negative values. To avoid this problem, it was constrained to be non-negative by the projected Landweber method, employing the following iterative algorithm

$$\begin{cases} Initialization : X_0 \\ y_{k+1} = X_k - \mu A^T (AX_k - b), \quad \mu = \frac{0.9}{\lambda_{max}(A^T A)} \\ X_{k+1} = \max(y_{k+1}, 0) \end{cases} \tag{21}$$

where the initialization for X_0 is given by the Tikonov method (equation (20)), $\lambda_{max}(A^T A)$ is the maximum eigenvalue of the square matrix $A^T A$, the step size parameter μ is chosen to reach convergence in a few iterations (5 iterations were considered here) and the maximum operator in the definition of X_{k+1} is evaluated component-wise.

To improve efficiency of the algorithm, the matrix A was fixed. Moreover, the matrix $M = (A^T A + \alpha I)^{-1} A^T$ (needed to compute the Tikonov solution), the matrix $A^T A$ and its maximum eigenvalue were computed before the application of the method to the signals. Thus, the algorithm required only a few matrix multiplications, which could be performed in real time.

This method has the limitation of requiring a preliminary phase, in which the waveforms representing the activity of different muscle regions are chosen. Moreover, it requires using high-density surface EMG detection systems with tens of electrodes. However, it is promising due to its low cost and the valuable output, decomposing the EMG into contributions from different muscle regions. By selecting the cross-sectional region corresponding to either the target or the crosstalk muscles, the two contributions could be separated (allowing both to quantify and to remove crosstalk).

An example of crosstalk quantification is shown in Figure 4. Simulated EMGs are considered. They were generated by two adjacent muscles and then summed. The signals were acquired by a linear array of electrodes placed in direction orthogonal to the fibres, covering both muscles. The algorithm for inverse modelling was applied (without imposing the non-negativity constraint, in order to better fit the data). The basis waveforms were SFAPs from fibres uniformly distributed in the cross-section covered by the two muscles. Then, the sources either on the left or on the right were considered to estimate the signals generated by either of the two muscles. The RMSs of the two estimated signals were used to quantify the amount of crosstalk. As the data were simulated, the estimation could be compared with the simulated signals. A good accord was obtained, even if the number of detection channels was quite small.

6 Conclusions

Crosstalk can pose limitations in many applications of surface EMG, when the activity of a specific muscle of interest is investigated. For many years, it was studied, showing how it was difficult to quantify and remove. Simulation models gave a fundamental contribution for its interpretation and have allowed to develop and test new ideas to face it. In most applications, researchers still rely on selective spatial filters to reduce it. However, this approach has limitations, as selecting the optimal filter is not possible without adapting to the specific case under investigation. Moreover, using very selective filters, there could be a problem of representativeness, as even the signal of the target muscle is largely discarded.

Recent approaches have been proposed to either estimate or reduce crosstalk. Some of them (e.g., BSS approaches) are quite difficult to implement and to run in real time. Maybe, for this reason, they didn't find many applications beyond the laboratory. However, some real time techniques have been proposed recently (e.g., OSTF, inverse modelling). They still have some limitations, as they require a preliminary phase in which the methods are fit to the specific conditions. Moreover, they were developed on theoretical basis and require tests in experimental conditions. However, they indicated a new promising

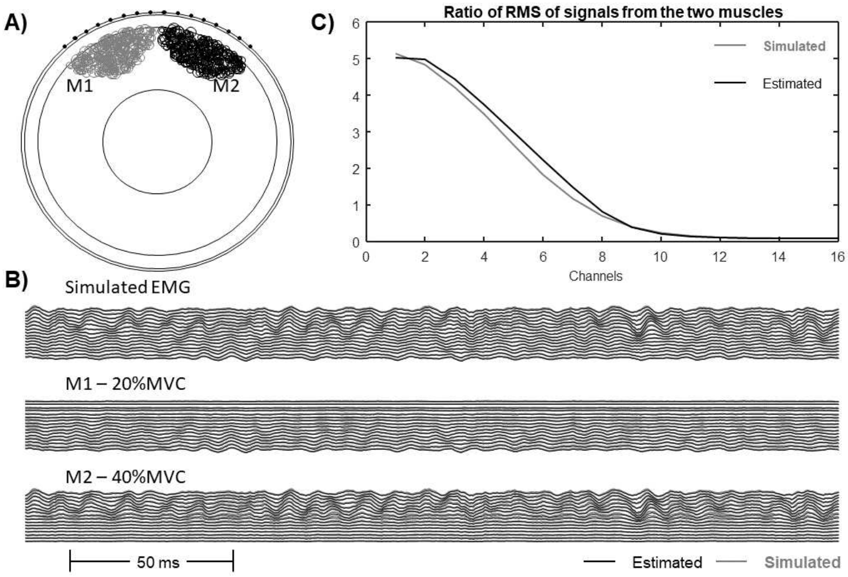

Fig. 4 Example of identification of muscle active regions to quantify crosstalk. A) A cylindrical volume conductor model (with radius of 50 mm) including bone, muscle, fat and skin tissues was used (same conductivities as for Figure 1, bone conductivity 20 mS/m). Single fibre potentials were simulated and summed-up to generate MUAPs (with MU dimensions given by the size of the circles). For each muscle, 400 MUs were simulated. Monopolar potentials were recorded by the indicated linear array of electrodes, placed transversally to the fibres, at 35 mm from the innervation zone (symmetrical fibres with semi-length 70 mm were simulated). B) Portion of simulated data (1 s of EMG was processed), considering the total signal and those generated by either of the two muscles. The simulated signals are superimposed to those estimated by inverse modelling based on 90 simulated fibres, uniformly distributed on the muscle regions (angle between $\pm 45^o$, depth between 1 and 9 mm). C) The contribution of crosstalk is quantified as the ratio between the RMS of the signals of the two muscles, either simulated or estimated.

path (basically, by stressing the importance of adapting to the investigated condition) that could be followed to deepen the research on crosstalk. Being also feasible for real time running on test data, they have the potential of being applied in the field in the near future.

Conflict of interest

The author declares that he has no conflict of interest.

References

1. Hug F (2011) Can muscle coordination be precisely studied by surface electromyography? J Electromyogr Kinesiol 21:1-12.

2. Jiang N, Englehart KB, Parker PA (2009) Extracting simultaneous and proportional neural control information for multiple-DOF prostheses from the surface electromyographic signal, IEEE Trans Biomed Eng 56 1070-80
3. Mitchell Barr K, Miller AL, Chapin KB (2010) Surface electromyography does not accurately reflect rectus femoris activity during gait: Impact of speed and crouch on vasti-to-rectus crosstalk, Gait & Posture 32:363-8.
4. Yong-Ku Kong, Hallbeck MS, Myung-Chul Jung (2010) Crosstalk effect on surface electromyogram of the forearm flexors during a static grip task, J Electromyogr Kinesiol 20:1223-9.
5. Mezzarane RA, Kohn AF (2009) A method to estimate EMG crosstalk between two muscles based on the silent period following an H-reflex, Med Eng Phys. 31:1331-6.
6. Lowery MM, Stoykov NS, Taflove A, Kuiken TA (2002) A multiplelayer finiteelement model of the surface EMG signal, IEEE Trans. Biomed. Eng. 49: 446-54.
7. Lowery MM, Stoykov NS, Dewald JP, Kuiken TA (2004) Volume conduction in an anatomically based surface EMG model, IEEE Trans. Biomed. Eng., 51: 2138-47
8. Mesin L (2008) Simulation of surface EMG signals for a multilayer volume conductor with a superficial bone or blood vessel. IEEE Trans Biomed Eng. 55:1647-57.
9. Mesin L, Smith S, Hugo S, Viljoen S, Hanekom T (2009) Effect of spatial filtering on crosstalk reduction in surface EMG recordings. Med Eng Phys 31:374-83.
10. Stoykov NS, Lowery MM, Kuiken TA (2005) A finite-element analysis of the effect of muscle insulation and shielding on the surface EMG signal. IEEE Trans Biomed Eng. 52:117-21.
11. Farina D, Merletti R, Indino B, Nazzaro M, Pozzo M (2002) Surface EMG crosstalk between knee extensor muscles: experimental and model results. Muscle Nerve 26:681-95.
12. Farina D, Arendt-Nielsen L, Merletti R, Indino B, Graven-Nielsen T (2003) Selectivity of spatial filters for surface EMG detection from the tibialis anterior muscle, IEEE Trans. Biomed. Eng. 50:354-64.
13. Farina D, Fvotte C, Doncarli C, Merletti R (2004) Blind separation of linear instantaneous mixtures of nonstationary surface myoelectric signals. IEEE Trans Biomed Eng. 51:1555-67.
14. Merletti R, De Luca CJ, Sathyan D (1994) Electrically evoked myoelectric signals in back muscles: Effect of side dominance, J. Appl. Physiol., 77:2104-14.
15. Talib I, Sundaraj K, Lam CK, Hussain J, Ali MA (2018) A review on crosstalk in myographic signals. Eur J Appl Physiol. 2018 Sep 21, Review.
16. De Luca CJ, Merletti R (1988) Surface myoelectric signal crosstalk among muscles of the leg. Electroencephalogr. Clin. Neurophysiol. 69:568-75.
17. Vieira TM, Botter A, Muceli S, Farina D (2017) Specificity of surface EMG recordings for gastrocnemius during upright standing. Sci Rep. 7(1):13300.
18. Mogk JPM, Keir PJ (2003) Crosstalk in surface electromyography of the proximal forearm during gripping tasks. J. Electromyogr. Kinesiol. 13:63-71.
19. Sinderby C, Friberg S, Comtois N, Grassino A (1996) Chest wall muscle cross talk in canine costal diaphragm electromyogram. J Appl Physiol (1985) 81(5):2312-27.
20. Frahm KS, Jensen MB, Farina D, Andersen OK (2012) Surface EMG crosstalk during phasic involuntary muscle activation in the nociceptive withdrawal reflex. Muscle Nerve. 46(2):228-36.
21. Solomonow M, Baratta R, Bernardi M, Zhou B, Lu Y, Zhu M, Acierno S (1994) Surface and wire EMG crosstalk in neighbouring muscles. J Electromyogr Kinesiol 4:131-42.
22. Campanini I, Merlo A, Degola P, Merletti R, Vezzosi G, Farina D (2007) Effect of electrode location on EMG signal envelope in leg muscles during gait, J Electromyogr Kinesiol 17:515-26.
23. Dimitrova NA, Dimitrov GV, Nikitin OA (2002) Neither high-pass filtering nor mathematical differentiation of the EMG signals can considerably reduce cross-talk, J Electromyogr Kinesiol, 12:235-46.
24. Lowery MM, Stoykov NS, Kuiken TA (2003) A simulation study to examine the use of cross-correlation as an estimate of surface EMG cross talk, Journal of Applied Physiology 94:1324-34.
25. De Luca CJ, Kuznetsov M, Donald Gilmore L, Roy SH (2012) Interelectrode spacing of surface EMG sensors: Reduction of crosstalk contamination during voluntary contractions, J Biomechanics 45:555-61.

26. Mesin L (2018) Optimal spatio-temporal filter for the reduction of cross-talk in surface electromyogram. J Neural Eng. 15(1):016013.
27. van Oosterom A (1998) Principles in inverse electrophysiological modelling, 6th Deliverable of the SENIAM project, 37-44.
28. Dimitrov GV, Disselhorst-Klug C, Dimitrova NA, Schulte E, Rau G (2003) Simulation analysis of the ability of different types of multi-electrodes to increase selectivity of detection and to reduce cross-talk, J. Electromyogr. Kinesiol. 13:125-38.
29. Disselhorst-Klug C, Silny J, Rau G (1997) Improvement of spatial resolution in surface-EMG: a theoretical and experimental comparison of different spatial filters, IEEE Trans. Biomed. Eng., 44:567-74.
30. Duchene J, Hogrel JY (2000) A model of EMG generation, IEEE Trans. Biomed. Eng., 47:192-201.
31. Mesin L, Cescon C, Gazzoni M, Merletti R, Rainoldi A (2009) A bi-dimensional index for the selective assessment of myoelectric manifestations of peripheral and central muscle fatigue, J Electromyogr. Kinesiol., 19:851-63.
32. Dimitrova NA, Dimitrov GV (2003) Interpretation of EMG changes with fatigue: facts, pitfalls, and fallacies, J. Electromyogr. Kinesiol. 13:13-36.
33. Roeleveld K, Blok JH, Stegeman DF, van Oosterom A (1997) Volume conduction models for surface EMG confrontation with measurements, J. Electromyogr. Kinesiol., 7:221-32.
34. Stegeman DF, Blok JH, Hermens HJ, Roeleveld K (2000) Surface EMG models: properties and applications, J. Electromyograph. Kinesiol. 10:313-26.
35. Shwedyk E, Balasubramanian R, Scott R (1977) A non-stationary model of the electromyogram, IEEE Trans. Biomed. Eng, 24:417-24.
36. Mesin L (2017) Mathematical Models for Biomedicine, ISBN: 9788892332980
37. Mesin L (2019) Neuromuscular System Engineering, ISBN: 9788892361881
38. Mesin L, Merletti R (2008) Distribution of electrical stimulation current in a planar multilayer anisotropic tissue. IEEE Trans Biomed Eng. 55(2 Pt 1):660-70.
39. Fuglevand AJ, Winter DA, Patla AE (1993) Models of recruitment and rate coding organization in motor-unit pools J. Neurophysiol. 70:2470-88
40. Farina D, Merletti R (2001) A novel approach for precise simulation of the EMG signal detected by surface electrodes, IEEE Trans. Biomed. Eng., 48:637-46.
41. Mesin L (2006) Simulation of Surface EMG Signals for a Multi-layer Volume Conductor with Triangular Model of the Muscle Tissue, IEEE Trans. Biomed. Eng., 53:2177-84
42. Farina D, Mesin L, Martina S (2004) Advances in surface EMG signal simulation with analytical and numerical descriptions of the volume conductor, Med. Biol. Eng. Comput., 42:467-76.
43. Mesin L, Joubert M, Hanekom T, Merletti R, Farina D (2005) A Finite Element Model for Describing the Effect of Muscle Shortening on Surface EMG, IEEE Trans. Biomed. Eng., 53:593-600.
44. Mesin L (2013) Volume conductor models in surface electromyography: Computational techniques, Comput. Biol. Med. 43:942-52
45. Mesin L (2013) Volume conductor models in surface electromyography: Applications to signal interpretation and algorithm test, Comput. Biol. Med., 43:953-61
46. Mesin L (2017) Introduction to Biomedical Signal Processing, ISBN: 9788892322721
47. Farina D, Mesin L, Martina S, Merletti R (2004) Comparison of spatial filter selectivity in surface myoelectric signal detection - Influence of the volume conductor model, Med. Biol. Eng. Comput., 42 114-120.
48. Mesin L, Kandoor AKR, Merletti R (2008) Separation of propagating and non-propagating components in surface EMG, Biomedical Signal Processing and Control, 3: 126-37.
49. Gallina A, Botter A (2013) Spatial localization of electromyographic amplitude distributions associated to the activation of dorsal forearm muscles. Front Physiol. 4:367.
50. Mesin L, Merletti R, Vieira TMM (2011) Insights gained into the interpretation of surface electromyograms from the gastrocnemius muscles: a simulation study, J. Biomech., 44:1096-103.
51. Vieira TMM, Loram ID, Muceli S, Merletti R, Farina D (2011) Postural activation of the human medial gastrocnemius muscle: are the muscle units spatially localised? J. Physiol. 589: 431-43.

52. Hodges PW, Gandevia SC (2000) Pitfalls of intramuscular electromyographic recordings from the human costal diaphragm. Clin Neurophysiol. 111(8):1420-4.
53. Kilner JM, Baker SN, Lemon RN (2002) A novel algorithm to remove electrical cross-talk between surface EMG recordings and its application to the measurement of short-term synchronisation in humans. J Physiol. 538(Pt 3):919-30.
54. Mesin L, Holobar A, Merletti R (2011) Blind source separation: application to biomedical signals. In: Cerutti S, Marchesi C (eds), Advanced methods of biomedical signal processing, IEEE Press series in biomedical engineering, John Wiley & Sons, pp 379-409.
55. Holobar A, Zazula D (2007) Multichannel Blind Source Separation Using Convolution Kernel Compensation. IEEE Trans. Signal Process. 55:4487-96.
56. Belouchrani A, Abed-Meraim K, Cardoso J-F, Moulines E (1997) A blind source separation technique using second-order statistics, IEEE Transactions on signal processing, 45(2):434–44.
57. Michel CM, Murray MM, Lantz G, Gonzalez S, Spinelli L, de Peralta RG (2004) EEG source imaging, Clinical neurophysiology, 115:2195-222.
58. Chauvet E, Fokapu O, Gamet D (2001) Inverse problem in the surface EMG: A feasibility study, in Proceedings of the 23rd Annual EMBS international Conference, Istanbul, Turkey, 1048-50.
59. Jesinger RA, Stonick VL (1994) Processing signals from surface electrode arrays for noninvasive 3D mapping of muscle activity, in IEEE DSP Workshop Prodceedings, 57-60.
60. LoPresti EF, Jesinger RA, Stonick VL (1995) Identifying Significant Frequencies in Surface EMG Signals for Localization of Muscle Activity, in IEEE EMBS Conference Proceedings, 967-8.
61. Mesin L (2015) Real time identification of active regions in muscles from high density surface electromyogram. Comput Biol Med. 56:37-50.
62. Roeleveld K, Stegeman DF, Vingerhoets HM, van Oosterom A (1997) The motor unit potential distribution over the skin surface, its use in estimating the motor unit location, Acta Physiol. Scand. 161:465-72.
63. Stonick JT, Jesinger RA, Stonick VL, Baumann SB (1996) Estimation and localization of multiple dipole sources for noninvasive mapping of muscle activity, IEEE Proceedings of the International Conference on Acoustics, Speech, and Signal Processing, 5:2912-5
64. van den Doel K, Ascher UM, Pai DK (2008) Computed myography: three dimensional reconstruction of motor functions from surface EMG data, Inverse Problems 24: 065010
65. van den Doel K, Ascher UM, Pai DK (2011) Source localization in electromyography using the inverse potential problem, Inverse Problems 27: 025008.